Long-Term Magnetic Resonance Imaging of Stem Cells in Neonatal Ischemic Injury

Andre Obenaus, PhD,[1,2,3,4] Nejmi Dilmac, PhD,[5] Beatriz Tone, BA,[2] Hou Rou Tian, MD,[2] Richard Hartman, PhD,[6] Murat Digicaylioglu, MD,[5] Evan Y. Snyder, MD, PhD,[5] and Stephen Ashwal, MD[2]

Objective: Quantitative magnetic resonance imaging (MRI) can serially and noninvasively assess the degree of injury in rat pup models of hypoxic ischemic injury (HII). It can also noninvasively monitor stem cell migration following iron oxide prelabeling. Reports have shown that neural stem cells (NSCs) may help mediate neuroprotection or stimulate neuroreparative responses in adult and neonatal models of ischemic injury. We investigated the ability of high-field MRI to monitor and noninvasively quantify the migration, proliferation, and location of iron oxide–labeled NSCs over very long time periods (58 weeks) in real time while contemporaneously correlating this activity with the evolving severity and extent of neural damage.

Methods: Labeled clonal murine NSCs (mNSCs) were implanted 3 days after unilateral HII in 10-day-old rat pups into the contralateral striatum or ventricle. We developed methods for objectively quantifying key aspects of dynamic NSC behavior (eg, viability; extent, and speed of migration; degree of proliferation; extent of integration into host parenchyma). MRI images were validated with histological and immunohistochemical assessments.

Results: mNSCs rapidly migrated (100 μm/day) to the lesion site. Chains of migrating NSCs were observed in the corpus callosum. In pups subjected to HII, though not in intact control animals, we observed a 273% increase in the MR-derived volume of mNSCs 4 weeks after implantation (correlating with the known proliferative behavior of endogenous and exogenous NSCs) that slowly declined over the 58-week time course, with no adverse consequences. Large numbers of now quiescent mNSCs remained at the site of injury, many retaining their iron oxide label.

Interpretation: Our studies demonstrate that MRI can simultaneously monitor evolving neonatal cerebral injury as well as NSC migration and location. Most importantly, it can noninvasively monitor proliferation dynamically for prolonged time periods. To be able to pursue clinical trials in newborns using stem cell therapies it is axiomatic that safety be insured through the long-term real time monitoring of cell fate and activity, particularly with regard to observing unanticipated risks to the developing brain. This study supports the feasibility of reliably using MRI for this purpose.

ANN NEUROL 2010;00:000–000

Neonatal brain hypoxic ischemic injury (HII) and ischemic perinatal stroke (IPS) remain frequent and devastating conditions with serious long-term sequelae of cerebral palsy, epilepsy, and mental retardation.[1,2] Current effective therapy has been limited to the immediate use of hypothermia in selected newborns with mild/moderate HII[3]; no other treatments have proven beneficial.

Several studies have demonstrated that neural stem cells (NSCs) improve behavioral[4–6] and anatomical[7–9] outcomes in adult and neonatal stroke/ischemia models when administered during a critical window after injury, suggesting that NSC implantation may offer an alternative treatment strategy for newborns. Previous studies have affirmed that murine[7] and human[10] NSCs, when

View this article online at wileyonlinelibrary.com. DOI: 10.1002/ana.22168

Received Jan 5, 2010, and in revised form Jul 3, 2010. Accepted for publication Jul 16, 2010.

Address correspondence to Andre Obenaus, Non-Invasive Imaging Laboratory, Departments of Radiation Medicine and Radiology, Loma Linda University, 11175 Campus St., CSPA1010, Loma Linda, CA 92324. E-mail: aobenaus@llu.edu or to Evan Y. Snyder, Sanford-Burnham Medical Research Institute, Program in Stem Cell & Regenerative Medicine, 10901 North Torrey Pines Road, La Jolla 92037; e-mail: esnyder@sanfordburnham.org

From the Departments of [1]Radiation Medicine, [2]Pediatrics, [3]Radiology, School of Medicine, Loma Linda University, Loma Linda, CA; Departments of [4]Biophysics and Bioengineering, [6]Psychology, School of Science and Technology, Loma Linda University, Loma Linda, CA; [5]Program in Stem Cell & Regenerative Biology, Sanford-Burnham Medical Research Institute, La Jolla CA.

Additional Supporting Information can be found in the online version of this article.

© 2010 American Neurological Association

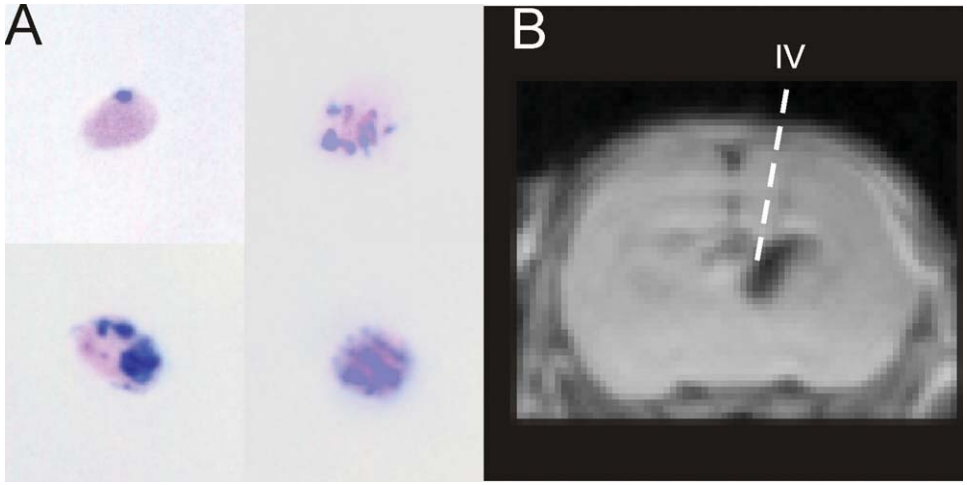

FIGURE 1: (A) Evaluation of iron labeling of murine C17.2 mNSCs by Prussian blue staining revealed that virtually all mNSCs had some iron particles, but with different levels of uptake. Using our 24-hour static incubation methods we were able to label >85% of all NSCs. (B) mNSCs were implanted under stereotactic guidance 3 days after induction of HII into either the contralateral ventricular system (shown) or striatal parenchyma. IV = intraventricular.

implanted 3–7 days post-HII, even at distances remote from injury, will migrate to and integrate within large regions of the infarcted hemisphere. Studies in neonatal mice also have demonstrated migration of intraventricular implanted NSCs (rodent and human) to the site of injury.[7,11,12]

Clinical application of neonatal stem cell treatment will require noninvasive tracking of cells to (1) demonstrate accuracy of implantation; (2) monitor cell migration, proliferation, and location; and (3) assess structural tissue recovery or, conversely, adverse host reactions. Several reports have demonstrated that iron-labeled NSCs can be tracked using magnetic resonance imaging (MRI)[13–15] but did not use MR evaluation for long periods of time (>6 months) and did not correlate NSC behavior with the dynamics of underlying pathology—critical for the actual translation of NSC-based therapeutics to patients.[7,11,16,17] The ability to monitor NSCs for extended periods is particularly important in newborns because long-term implantation may pose unanticipated risks to the developing brain.

We investigated whether high-field MRI could track migration and location of iron-labeled NSCs for greater than 1 year in relation to the shifting functional landscape of the damaged newborn brain. In addition to detection of NSCs for at least 58 weeks, we also developed methods to objectively quantify key aspects of dynamic NSC behavior (eg, viability, extent/speed of migration, degree of proliferation, integration into host parenchyma).

Subjects and Methods

Animal Model of HII

HII was induced using a modified Rice-Vannucci model (RVM) of unilateral common carotid artery occlusion with hypoxia exposure to a gas mixture of 8% O_2 balanced with N_2 (according to Ashwal and colleagues[18]) in unsexed 10-day-old Sprague-Dawley rat pups. The right common carotid artery was exposed and ligated and allowed to recover for 2 hours with the dam. Hypoxia was induced by placing pups in a jar containing a humidified gas mixture (8% O_2-balance N_2) for 1.5 hours and maintained at 37°C. Animals were randomly assigned into 3 groups, controls (no HII), HII with parenchymal NSC implantation, and HII with intraventricular implantation (n = 6), and all animals were imaged over the 58-week experimental time line (see Neuroimaging).

NSC Maintenance, Labeling, and Implantation

For implantation, we employed NSCs derived from mice. To model NSC behavior, we used early passages of a stable clonal population of dependably engraftable *lacZ*-expressing mouse NSCs (mNSCs) grown as homogenous, cell cycle–synchronized and differentiation state–synchronized monolayers. The clonal mNSCs were taken from a well-characterized clone, C17.2,[7,19–21] because of their enhanced yet constitutively self-regulated self-renewal[7,19] and expression of a "stem" genetic profile.[22,23] NSCs were maintained as previously described.[7] Upon reaching 90% confluence cultured monolayers of mNSCs were trypsinized, washed, and gently triturated into a single-cell suspension for electroporation with 50 μl of Feridex solution (Feridex; Berlex Imaging, Wayne, NJ; 11.2 mg Fe/ml) (see Supporting Information). Feridex was actively/passively transported into the *lacZ*-expressing mNSCs (Fig 1). An alternative labeling strategy entailed incubating freshly trypsinized mNSCs for 24 hours with Feridex (30 μg/ml) (see Fig 1A; and see Supporting Information for additional NSC details).

At 3 days post-HII induction, labeled NSCs were implanted into 2 locations contralateral to the lesion (ventricle and striatum) as previously described.[7] Under isoflurane anesthesia, a small burr hole was drilled and a glass micropipette containing 5 μl of a freshly trypsinized mNSC suspension

(500,000 mNSCs) was slowly inserted under stereotactic guidance into the striatum or ventricle (1 μl/minute for 5 minutes) (see Fig 1B). Control animals that did not undergo HII received mNSCs into the same hemisphere/ventricle as the HII pups (see Supporting Information).

Neuroimaging

Pups were lightly anesthetized (isoflurane 3% induction, 1.0% maintenance)[18] and MR data were collected on a Bruker Advance 11.7T MRI (8.9-cm bore) using a 10-echo T2 sequence (TR/TE = 4600 msec/10.2 msec; matrix size = 256 × 256; field of view [FOV] = 3 cm) followed by a diffusion-weighted sequence (TR/TE = 3000 msec/25 msec; b-values = 0.72 seconds/mm^2 and 1855.64 seconds/mm^2), matrix size = 128 × 128; FOV = 3 cm) that encompassed the entire brain. At 3 to 4 weeks of age the pups were imaged on a larger bore Bruker 4.7T (30 cm) imager using identical imaging parameters. Serial MRI was performed at −3 days (1 day post RVM), 1 day (1 day postimplantation), and 1, 2, 3, and 4 weeks, then once monthly for 58 weeks for all animals in the study.

T2-weighted images (T2WI) and diffusion-weighted images (DWI) were used to evaluate regions of hypointensity (mNSCs) or hyperintensity (HII) to delineate mNSCs or regions of HII. Corresponding lesion and NSC volume data were extracted. Analysis included HII volume, non-HII brain volume, NSC volume, and total brain volume. A signal intensity threshold 1.25 times lower than the surrounding tissue mapped the labeled mNSCs. Migration was assessed by measuring the leading edge of the hypointensity on T2WI at the level of implantation (contralateral intraventricular or parenchymal) on successive temporal imaging datasets. Measured NSC volume over time for each animal was normalized to brain volume and averaged across all animals for each group (intraventricular or parenchymal). This calculated proliferation index (CPI) measured the NSC volume in control and ischemic NSC implanted pups. An area under the curve (AUC) analysis was used to obtain a relative real-time noninvasive measure of proliferation and was found to be consistent with the bromodeoxyuridine (BrdU) incorporation data obtained using these same mNSCs implanted in the same manner in the same newborn mouse RVM HII model[7] (see Supporting Information for additional details).

Histology and Immunohistochemistry

At 58 weeks, all animals were euthanized and perfused transcardially with 4% paraformaldehyde followed by cryoprotection sectioning (30 μm serial sections). Cresyl violet acetate[18] and Prussian blue iron staining were used to assess cellular health and iron-labeled cells. Fluorescent immunohistochemistry used floating sections for *lacZ* as assessed by anti-β-galactosidase (βgal) or standard X-gal histochemistry, as described previously.[7] The anti-β-gal was a polyclonal antibody raised in rabbits (Cappel; 1:1000) while the secondary antibodies were FITC-conjugated goat anti-mouse immunoglobulin G (IgG; Vector Laboratories), 1:200 and Texas red (TR)-conjugated horse anti-rabbit IgG (Vector; 1:200). Control sections omitted the primary antibody and/or used an irrelevant antibody. Immunolabeled slides were scanned on a confocal microscope (BioRad 1024) with a Z-series of 10–12 images collected by stepping through ~1-μm sections for each tissue. For immunohistochemistry combined with hematoxylin and eosin (H&E) histology, brain sections were treated identically as above. Neuronal tract tracing utilized biotinylated-dextran–fluorescein isothiocyanate (BDA-FITC) (0.4μl of 10% BDA-FITC dissolved in double-distilled water [ddH_2O]) as described[24] (see Supporting Information).

Behavior

Testing consisted of a series of tasks designed to assess a wide variety of behavioral domains, including cognitive (water maze), activity levels (open field), and sensorimotor coordination (rotarod) that were administered at 3, 8, and 12 months after NSC implantation (see Supporting Information)

Results

Long-Term Imaging of the HII Lesion in Relation to Exogenous NSCs

We examined the evolution of HII lesion volume as well as migration, proliferation, and long-term persistence of mNSCs in relation to the lesion.

EVOLUTION OF ISCHEMIC INJURY OVER 58 WEEKS. Initially (day 1), lesion volume (regions of hyperintensity) was 40% of the hemisphere and over the first week decreased to <15% (Fig 2A, B, C). Imaging abnormalities encompassed ipsilateral striatal and cortical regions.[18] Imaging abnormalities then increased, with most of the striatum being affected along with varying degrees of the cortex. The affected tissue volume slowly increased to ~35% by 16 weeks and remained stable to 58 weeks (see Fig 2C).

QUANTIFICATION OF MNSC VOLUMES. 3D assessment of mNSC volumes in transplanted but uninjured controls showed that there was a slow and steady decrease by 80% over 58 weeks (see Fig 2B, D). In contrast, in RVM animals (ventricular or striatal implantation), there was a 273% increase in apparent mNSC volumes over the first 4 weeks postimplantation when the mNSC volumes were normalized to brain volume (see Fig 2D). While there was moderate variability between animals, the average peak increase occurred ~3 weeks postimplantation. After this increase, there was gradual decline (to 72% of initial volume) over 58 weeks. At 4, 12, 31, and 58 weeks the mNSC volume was 239%, 115%, 85%, and 53% larger than controls, respectively. These results support the histological findings that many of these newly-born neural cells fail to survive long-term, leaving ~20% of the new neural cells that have incorporated into the penumbral region, contributing to new parenchyma,[24] and reflected in the 53% larger volume of mNSCs ultimately seen in injured areas compared to

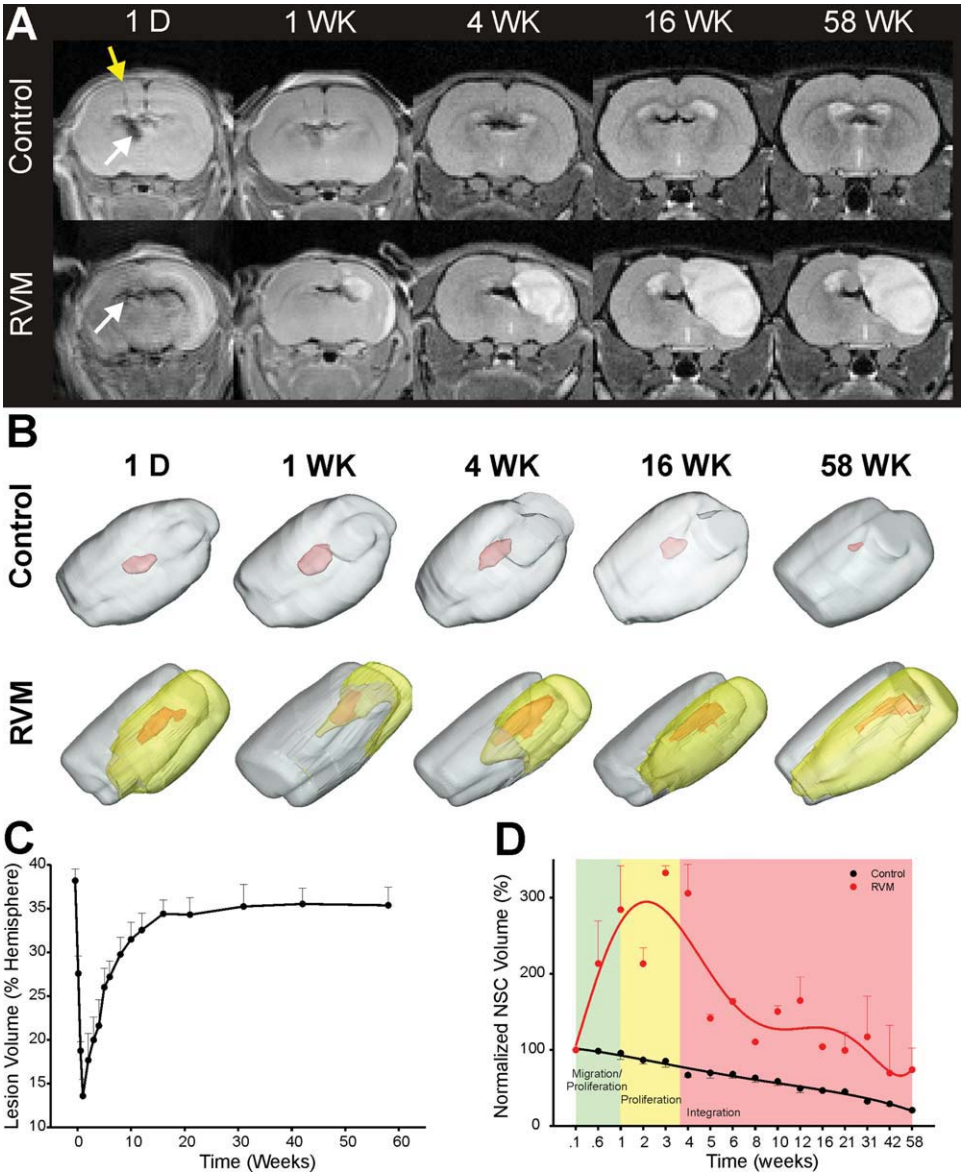

FIGURE 2: Neuroimaging of mNSC implantation. (A) Serial T2WI shows hypointense (dark) areas corresponding to the implantation *(yellow arrow)* of iron-labeled cells that remain within the ventricular system of control animals whereas cells migrate rapidly and enter HII regions in the RVM rodents. We were able to detect iron-labeling even at 58 weeks. (B) 3D volumetric reconstruction of T2WI data illustrates the implanted mNSC migration and distribution over the 58-week observation period. NSCs remain detectable in control and RVM animals even though cell volumes were diminished at 58 weeks; *yellow* = HII volume, *red* = mNSC volume. (C) Temporal changes in RVM lesion volume shows a 40% lesion volume (% of hemisphere) that by 1 week reaches a minimum volume of 15%, which then continues to increase slowly over the next 16 weeks and plateaus for the remainder of the 58 weeks. (D) Calculation of the normalized (to hemispheric volume) mNSC volume, revealed that in all control animals (not expected to proliferate) there was a steady decline over the 58 weeks. In contrast, the RVM animals (expected to proliferate) revealed a rapid increase (~300%) in mNSC volume over the first 4 weeks after implantation that then slowly declined to a similar mNSC volume noted at the time of implantation.

uninjured non-neurogenic regions (neoplasms, cell overgrowth, or cytoarchitectural distortion was never observed). All iron-containing mNSC-derived cells ultimately studied after 1 year were viable and integrated.

MIGRATION. Migration (distance from injection site) was assessed in uninjured control and RVM pups beginning 1 day after implantation and serially to 4 weeks. In controls without ischemia, mNSCs by and large did not migrate extensively from their point of implantation based on persistence of T2WI hypointensities at the implantation site (see Fig 2A). By contrast, in RVM animals, mNSCs migrated from the ventricle or striatum toward the ischemic lesion over 58 weeks; few mNSCs remained at the implantation site (see Fig 2A). striatally implanted mNSCs migrated at about 100–125 μm/day

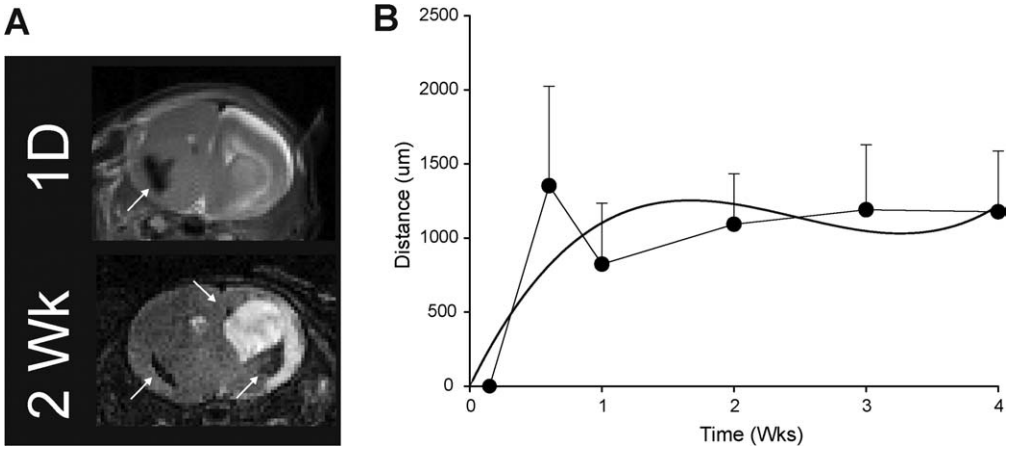

FIGURE 3: NSC migration rates. Migration rates were determined by measuring the leading edge of NSCs as they migrated through tissue. NSCs migrate rapidly at about 100 μm per day for the first few days after implantation and presumably are extralesional. Migration then plateaus when NSCs are presumably intralesional. Curves were generated using a Euclidean function. The data were curve fitted to estimate overall migrational distances *(solid curved line)*.

through tissues to the outermost border of the HI lesion (Fig 3). Based on MR images and using either Euclidian or Manhattan metrics, we ascertained that the first Feridex-labeled mNSCs arrived at the site of injury within 4–7 days. Curve fitting of the data suggested that the average peak migration time to the lesion occurs within 10–12 days postimplantation. By 2 weeks, all animals with an RVM lesion had NSCs that were MR-visible within or adjacent to the area of HII. Migration rates could not be further assessed after the first 3–4 weeks as the leading edge of the hypointensity was within or in contact with the HII lesion.

LABELED MNSCS REMAIN VISIBLE AT 58 WEEKS POSTIMPLANTATION. We were able to visualize labeled mNSCs in control and RVM animals for at least 58 weeks postimplantation (Fig 4). Although there was variability in the amount of iron within each mNSC and the amount of labeling per cell decreases by 50% with each cell division,[25] the degree of labeling and the volume of cells we derived were optimal for MRI to serially detect most NSCs for >1 year (see Fig 4A). In control animals, whether implantation was into the ventricle or striatum, we found little evidence of migration; nevertheless, iron-labeled mNSCs could be detected at their original site of injection. In RVM animals, where migration was robust, labeled mNSCs could be monitored using MRI at sites distant from implantation, typically adjacent to the ischemic lesion (see Fig 4B; Fig 5). Extensive migration was more characteristic of animals that had ventricular rather than striatal implantation.

Most importantly, in control and RVM animals, the hypointense MR signals correlated histologically with the location of these iron-labeled cells (see Fig 4A, B), suggesting that T2WI MRI can identify the location of implanted mNSCs when they are labeled, even at 58 weeks.

Histological and Immunohistochemical Correlation

Validation of mNSC location at 58 weeks by immunolabeling demonstrated mNSCs in the vicinity of the lesion (see Fig 5A, B). Implanted Feridex-labeled mNSCs were present at the periphery of the cavitated cystic HI injury and were the same cells traced by MRI over the 1-year course (see Fig 5C, E) and were found in multiple sites often between the site of implantation and injury (see Fig 5D). Immunolabeled stem cells were observed in and around the lesion as bands of mNSCs or as large perilesional clusters (see Fig 5E). Similar findings were seen using immunoperoxidase histochemistry with clusters in the parenchyma and large numbers of β-gal+ cells adjacent to the glial scar of the lesion (see Fig 5H, asterisk). As shown in Figure 5F, we observed strong BDA staining from the cortical injection site to the lesion.

Histological evaluation of uninjured controls confirmed the MRI-based conclusion that implanted mNSCs had not migrated from their site of injection; as demonstrated by MRI (see Fig 2A, B). β-gal+ cells (that were also Prussian blue+) were present only within the ventricular system (data not shown). Also as shown by MRI, even at 58 weeks, chain-like groups of mNSCs throughout the brain were only detected in injured animals (see Fig 5H). These chains were often in the corpus callosum (see Fig 5G) or adjacent to the injury, and, in some cases, were associated with clusters of mNSCs (see Fig 5H).

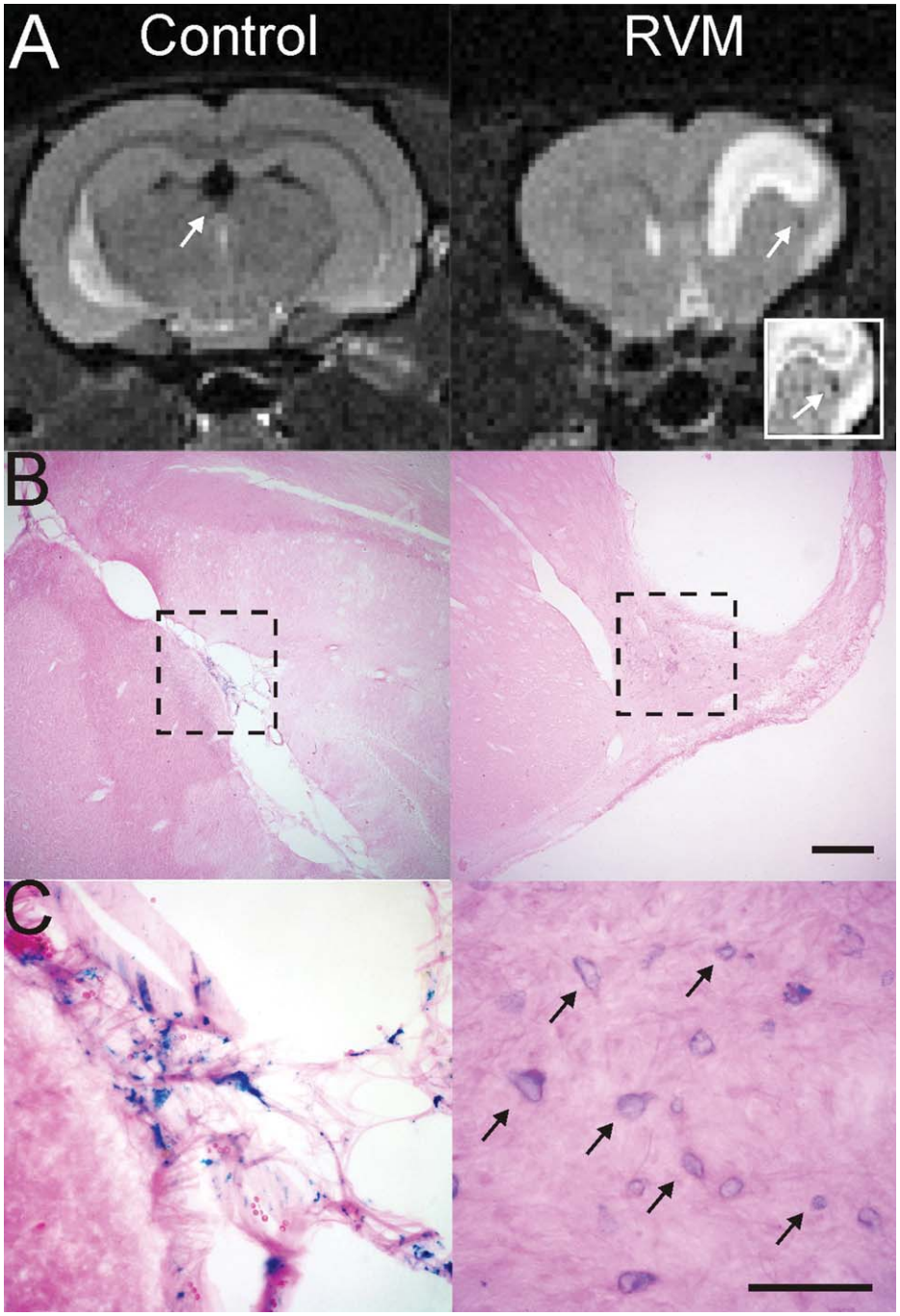

FIGURE 4: Iron-oxide–labeled NSCs are still visible on MRI at 58 weeks. (A) A control animal implanted with NSCs within the ventricle still exhibits MRI hypointensities within the ventricle *(arrow)* at 58 weeks after implantation. An RVM animal that had an intrastriatal implantation of NSCs clearly shows an MR-visible hypointensity adjacent to the lesion *(arrow)*. Inset clearly identifies a loss of T2 signal *(arrow)* adjacent to the lesion site. (B) A histological section from the control animal shows no lesion but iron-labeled mNSCs within the ventricle. In contrast, the RVM animal has iron-labeled mNSCs adjacent to the lesion. Bar = 0.5 mm. (C) A high-power photomicrograph (40×) allows clear visualization of iron-labeled cells *(arrows)* still within the choroid plexus of the ventricle even at 58 weeks, whereas the mNSCs are neighboring the lesion in the RVM animals. Bar = 100 μm.

The neural cell types into which the mNSCs differentiated were comparable to those previously reported by us[7] and others[26] for this type of stem cell in this type of disease: ~5% of NSCs differentiated toward neuronal lineages with the remaining viable cells differentiating into oligodendrocytes (~4%) or astrocytes (~30%), and the remainder being undifferentiated, quiescent neural progenitors.

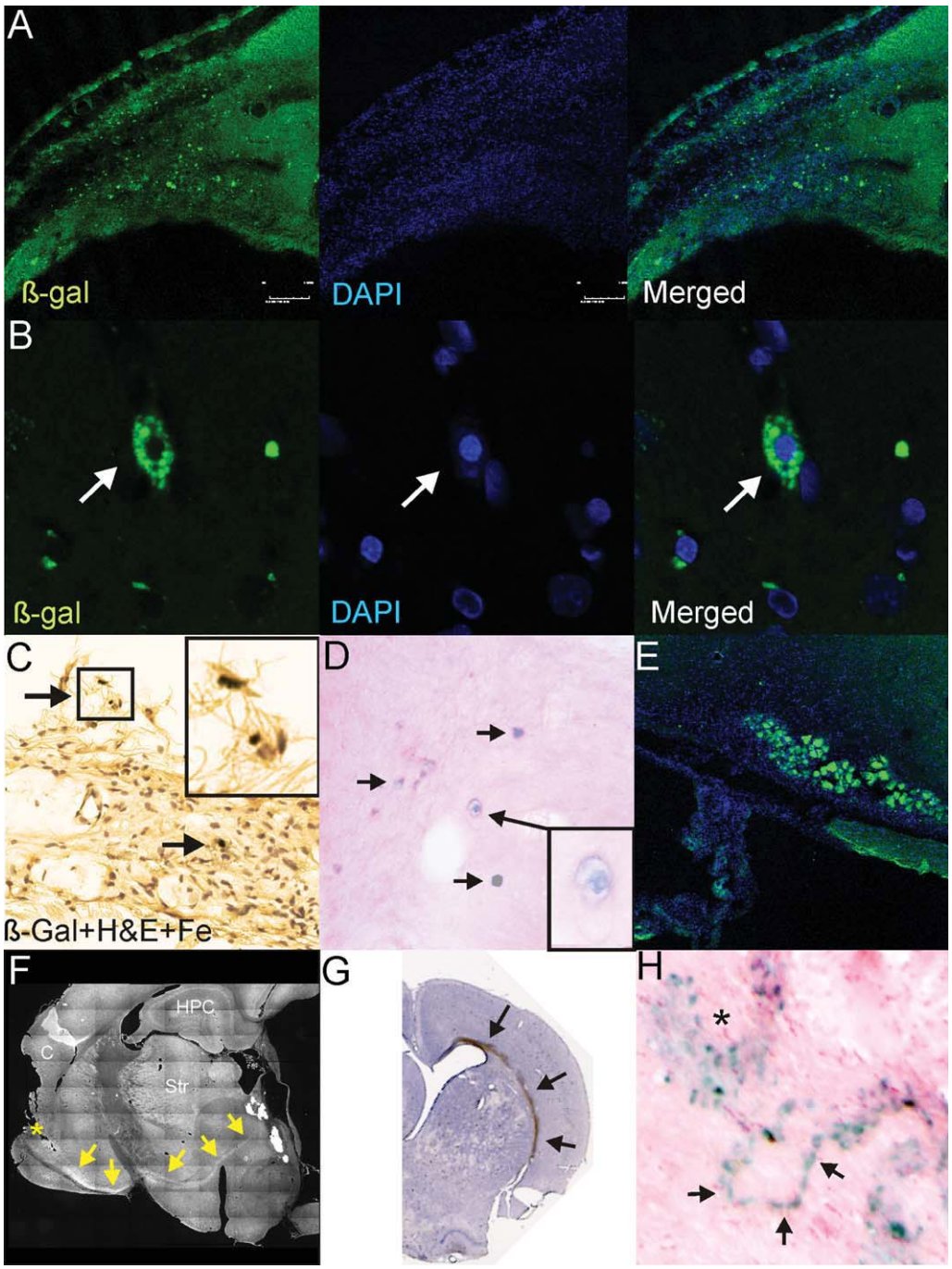

FIGURE 5: Immunohistochemical and histological assessment of NSCs at 58 weeks after implantation. (A) Dual-labeled fluorescent staining revealed that numerous *β*-gal–positive cells could be observed in the vicinity of the ischemic lesion. (B) High power (100×) examination of these cells revealed that *β*-gal was localized within the cytoplasm and these cells were healthy with DAPI staining in the nucleus. (C) Similarly, at more ventral locations, similar iron-stained and *β*-gal–stained cells could be observed *(arrows)*. Inset: High-power magnification illustrates iron-containing cells. (D) Prussian blue staining followed by H&E counterstaining also demonstrates numerous iron-containing cells within the parenchyma adjacent to the injured tissues. (E) In many sites adjacent to the lesion, large groups of *β*-gal–stained cells could be observed, suggesting the possibility that many of these cells may replicate in the vicinity of the injury. (F) BDA injection (*) in a subset of animals revealed unusual anterograde transport within the brains of these animals. The appearance of a robust stained pathway at the base of the striatum was noted. (G) Gross histological specimen showing robust staining within the corpus callosum of an animal following parenchymal injection at 58 weeks after implantation. Robust *β*-gal–positive staining could be observed on the side of the HII injury. (H) Similarly, even with Prussian blue staining, numerous clusters (*) of iron-labeled NSCs could be observed, but chain-like series of iron-labeled cells could also be seen. DAPI = 4′,6-diamidino-2-phenylindole.

Concerns have at times been voiced that implanted iron-containing mNSCs might worsen symptomatology. Reassuringly, on motor, spatial, learning, and memory tasks, the deficits in RVM mice transplanted with iron-labeled mNSCs were no more significant than in control RVM mice (see Supporting Information).

Discussion

Noninvasive real-time imaging modalities, such as MRI, will play a critical role in the clinical application of stem cell therapy across the spectrum of human age and disease, particularly in the central nervous system (CNS), which is otherwise inaccessible to visual inspection.[27,28] Such monitoring likely will be mandatory for clinical trials that precede acceptance for routine therapy, given that such trials will focus on insuring long-term safety of cell-based interventions. MRI provides the ability to assure targeted implantation, track migration and cell-host interactions, validate and quantify reparative responses, monitor cell proliferation, and assess any adverse impacts on host parenchyma and vasculature. The latter 2 functions may be critical for knowing when to trigger a suicide gene within the transplanted NSCs, a likely requirement by most regulatory agencies. Our current study provides a framework for such translational research, using as proof-of-principle, NSCs in neonatal HII, a plausible early target for stem cell-based therapies. Our study was not designed to investigate the therapeutic effectiveness of NSCs but rather to evaluate whether NSCs rendered "visible" to MRI with iron-labeling could be effectively and safely visualized and monitored for extended time periods without adversely altering either stem cell behavior, status of the host to support engraftment, or the baseline disease condition. Furthermore, the success of murine NSCs to remain viable within the rat brain is well known.[29,30]

Animals subjected to HII and followed long-term (for 58 weeks) did evince significant behavioral deficits due to ongoing cavitation of the lesion (see Fig 2C), but this effect was not worsened by NSCs and NSCs implanted into uninjured animals did not create behavioral, functional, or histological problems. The purpose of the study was one of visualization of NSCs and *not* of optimizing NSC dose, time of administration, location of administration(s), number of cotemporaneous or sequential administrations, adjunctive agents, or accompanying motor and cognitive enrichment for optimal therapeutic benefit. Indeed, the NSCs were *not* implanted into a region that would likely have yielded optimal benefit—directly in the penumbra (by virtue, in part, of their known anti-inflammatory, anticavitation actions). Rather, the NSCs were administered *distant* from the lesion to be able to determine whether MRI could track and quantify the dynamic of their migration and proliferation. However, with the knowledge that MRI can be used in this regard and that iron-labeling of NSCs is safe and will not alter the profile of the disease itself, in future studies parameters for maximizing efficacy and benefit can now be systematically tested—in a noninvasive manner in real-time for a given subject within a large cohort of animals where intermittent or repeated treatment in multiple locations might be feasible.

Long-Term Detection of Viable mNSCs by MRI

This is the first report to document the ability of MRI to monitor iron-labeled NSCs in a model of neonatal HII for up to 58 weeks, essentially the lifespan of a laboratory rat. While it is known that NSCs can be visualized using MRI as they migrate to the injury site,[5,7,25,31] the majority of studies have been of relatively short duration.[32–37] The one long-term follow-up study[38] did not involve the developing neonatal brain, which is an entirely different CNS "terrain." Indeed, a number of adult studies suggest that implanted stem cells may *not* retain their iron label.[39] While more study is required to harmonize the results from disparate studies, differences in iron-labeled compounds, injury models, imaging methods, time points, and histological endpoints combined with age-related changes likely account for the variability with regard to long-term visualization of NSC within the brain. We describe a method by which NSCs (based on signal voids on T2 imaging) could be monitored accurately throughout the 58-week period as confirmed by histology. Indeed, the MRI resolution may have been good enough to detect small clonal populations of NSCs (see Fig 5).

MR susceptibility studies have suggested that MRI may not only overestimate the hypointensity on T2 or other imaging modalities[40] but also the number of iron-labeled NSCs seen on MR could be an overrepresentation of the actual number of NSCs present.[9,41] In our study we observed greater MRI hypointensities than that seen with Prussian Blue staining and future histological studies will need to be correlated to the loss of MR signal. The return of NSC volume to control levels could be the result of numerous processes, including: (1) loss of detection limits by MRI, (2) migration of NSC-derived cells away from the region of initial integration, and (3) discharge (and hence loss) of iron particles during proliferation and/or cell death. While other potential explanations remain plausible, the most likely explanation is that the system prunes cells over time that are no longer necessary for the repair process and/or have not made

synaptic connections or have simply become senescent. Stereological criteria were utilized to determine cellular densities from MR-based images, similar to those from histological results.[42,43]

Monitoring Migration over Long Time Periods

Using MRI, it was possible to calculate the speed at which these NSCs migrate in the injured neonatal brain.[6,44–46] Migration occurred within 4–10 days at ~100–125μm/day. This rate is almost double that seen in adult brains,[47–49] information that is important for planning newborn stem cell–based trials. Given that it is widely acknowledged that a relatively narrow "window-of-opportunity" for neuroprotection or neural repair exists after ischemic injury—typically within the first 10 days—it is significant that potentially reparative NSCs might engage the injury site more quickly and in greater numbers within that "window" in the developing than in the adult brain. Water content is higher and tissue density/compactness lower in the developing mammalian brain and may provide less of a structural barrier to cell movement within parenchymal tissues.[50,51] Knowledge of such a tempo may provide guidance as to how often and when to monitor for adverse events.

Monitoring Proliferation over Long Time Periods

One of our more useful (and novel) findings is that the volume of T2 hypointensities could provide a real-time noninvasive surrogate measure for cell proliferation by calculating a "proliferation index" (CPI). These inferences were entirely consistent with the known dynamics of BrdU incorporation using the same mNSCs implanted in the same manner in the same newborn mouse RVM HII model.[7] Such monitoring will be critical during any clinical use of NSCs.

NSC Viability and Location

Another important consideration is the early loss of a portion of NSCs after implantation. Several studies have suggested that up to 50% of implanted cells may be lost[11,52,53] via toxic inflammatory molecules, free radicals, excess intracellular calcium, and excess extracellular glutamate in response to the initial injury.[54] However, when implanted during the proper postinjury interval, NSCs appear to survive and flourish. Our data suggest that MRI might be used to ascertain the appropriate time points for implantation following injury.

Acknowledgments

This research was supported by grants from the Department of Pediatrics, Non-Invasive Imaging Laboratory, Loma Linda University; and the NIH NINDS (1RO1NS059770-01A2).

We thank G. McAuley for the initial migration calculations.

Potential conflict of interest

Nothing to report.

References

1. Dilenge ME, Majnemer A, Shevell MI. Long-term developmental outcome of asphyxiated term neonates. J Child Neurol 2001;16: 781–792.
2. Raju TN, Nelson KB, Ferriero D, Lynch JK. Ischemic perinatal stroke: summary of a workshop sponsored by the National Institute of Child Health and Human Development and the National Institute of Neurological Disorders and Stroke. Pediatrics 2007; 120:609–616.
3. Gluckman PD, Wyatt JS, Azzopardi D, et al. Selective head cooling with mild systemic hypothermia after neonatal encephalopathy: multicentre randomised trial. Lancet 2005;365:663–670.
4. Roberts TJ, Price J, Williams SC, Modo M. Preservation of striatal tissue and behavioral function after neural stem cell transplantation in a rat model of Huntington's disease. Neuroscience 2006; 139:1187–1199.
5. Sykova E, Jendelova P. Migration, fate and in vivo imaging of adult stem cells in the CNS. Cell Death Differ 2007;14:1336–1342.
6. Ben-Hur T, van Heeswijk RB, Einstein O, et al. Serial in vivo MR tracking of magnetically labeled neural spheres transplanted in chronic EAE mice. Magn Reson Med 2007;57:164–171.
7. Park KI, Hack MA, Ourednik J, et al. Acute injury directs the migration, proliferation, and differentiation of solid organ stem cells: evidence from the effect of hypoxia-ischemia in the CNS on clonal "reporter" neural stem cells. Exp Neurol 2006;199:156–178.
8. Bulte JW, Duncan ID, Frank JA. In vivo magnetic resonance tracking of magnetically labeled cells after transplantation. J Cereb Blood Flow Metab 2002;22:899–907.
9. Walczak P, Zhang J, Gilad AA, et al. Dual-modality monitoring of targeted intraarterial delivery of mesenchymal stem cells after transient ischemia. Stroke 2008;39:1569–1574.
10. Imitola J, Raddassi K, Park KI, et al. Directed migration of neural stem cells to sites of CNS injury by the stromal cell-derived factor 1alpha/CXC chemokine receptor 4 pathway. Proc Natl Acad Sci U S A 2004;101:18117–18122.
11. Park KI, Himes BT, Stieg PE, et al. Neural stem cells may be uniquely suited for combined gene therapy and cell replacement: evidence from engraftment of neurotrophin-3-expressing stem cells in hypoxic-ischemic brain injury. Exp Neurol 2006;199:179–190.
12. Comi AM, Cho E, Mulholland JD, et al. Neural stem cells reduce brain injury after unilateral carotid ligation. Pediatr Neurol 2008; 38:86–92.
13. Modo M, Roberts TJ, Sandhu JK, Williams SC. In vivo monitoring of cellular transplants by magnetic resonance imaging and positron emission tomography. Expert Opin Biol Ther 2004;4: 145–155.
14. Lepore AC, Walczak P, Rao MS, et al. MR imaging of lineage-restricted neural precursors following transplantation into the adult spinal cord. Exp Neurol 2006;201:49–59.
15. Guzman R, Uchida N, Bliss TM, et al. Long-term monitoring of transplanted human neural stem cells in developmental and pathological contexts with MRI. Proc Natl Acad Sci U S A 2007;104: 10211–10216.

16. Bulte JW, Arbab AS, Douglas T, Frank JA. Preparation of magnetically labeled cells for cell tracking by magnetic resonance imaging. Methods Enzymol 2004;386:275–299.

17. Stroh A, Faber C, Neuberger T, et al. In vivo detection limits of magnetically labeled embryonic stem cells in the rat brain using high-field (17.6 T) magnetic resonance imaging. Neuroimage 2005;24:635–645.

18. Ashwal S, Tone B, Tian HR, et al. Comparison of two neonatal ischemic injury models using magnetic resonance imaging. Pediatr Res 2007;61:9–14.

19. Parker MA, Anderson JK, Corliss DA, et al. Expression profile of an operationally-defined neural stem cell clone. Exp Neurol 2005; 194:320–332.

20. Snyder EY, Deitcher DL, Walsh C, et al. Multipotent neural cell lines can engraft and participate in development of mouse cerebellum. Cell 1992;68:33–51.

21. Jaderstad J, Jaderstad LM, Li J, et al. Communication via gap junctions underlies early functional and beneficial interactions between grafted neural stem cells and the host. Proc Natl Acad Sci U S A 2010;107:5184–5189.

22. Cartwright P, McLean C, Sheppard A, et al. LIF/STAT3 controls ES cell self-renewal and pluripotency by a Myc-dependent mechanism. Development 2005;132:885–896.

23. Murphy MJ, Wilson A, Trumpp A. More than just proliferation: Myc function in stem cells. Trends Cell Biol 2005;15:128–137.

24. Park KI, Teng YD, Snyder EY. The injured brain interacts reciprocally with neural stem cells supported by scaffolds to reconstitute lost tissue. Nat Biotechnol 2002;20:1111–1117.

25. Walczak P, Kedziorek DA, Gilad AA, et al. Applicability and limitations of MR tracking of neural stem cells with asymmetric cell division and rapid turnover: the case of the shiverer dysmyelinated mouse brain. Magn Reson Med 2007;58:261–269.

26. Hicks AU, MacLellan CL, Chernenko GA, Corbett D. Long-term assessment of enriched housing and subventricular zone derived cell transplantation after focal ischemia in rats. Brain Res 2008; 1231:103–112.

27. Ashwal S, Obenaus A, Snyder EY. Neuroimaging as a basis for rational stem cell therapy. Pediatr Neurol 2009;40:227–236.

28. Obenaus A, Ashwal S. Magnetic resonance imaging in cerebral ischemia: focus on neonates. Neuropharmacology 2008;55: 271–280.

29. Klassen H, Lund RD. Retinal transplants can drive a pupillary reflex in host rat brains. Proc Natl Acad Sci U S A 1987;84:6958–6960.

30. Irons H, Lind JG, Wakade CG, et al. Intracerebral xenotransplantation of GFP mouse bone marrow stromal cells in intact and stroke rat brain: graft survival and immunologic response. Cell Transplant 2004;13:283–294.

31. Chang NK, Jeong YY, Park JS, et al. Tracking of neural stem cells in rats with intracerebral hemorrhage by the use of 3T MRI. Korean J Radiol 2008;9:196–204.

32. Sykova E, Jendelova P. In vivo tracking of stem cells in brain and spinal cord injury. Prog Brain Res 2007;161:367–383.

33. Kameda M, Shingo T, Takahashi K, et al. Adult neural stem and progenitor cells modified to secrete GDNF can protect, migrate and integrate after intracerebral transplantation in rats with transient forebrain ischemia. Eur J Neurosci 2007;26:1462–1478.

34. Panizzo RA, Kyrtatos PG, Price AN, et al. In vivo magnetic resonance imaging of endogenous neuroblasts labelled with a ferumoxide-polycation complex. Neuroimage 2009;44:1239–1246.

35. Magnitsky S, Watson DJ, Walton RM, et al. In vivo and ex vivo MRI detection of localized and disseminated neural stem cell grafts in the mouse brain. Neuroimage 2005;26:744–754.

36. Wennersten A, Meier X, Holmin S, et al. Proliferation, migration, and differentiation of human neural stem/progenitor cells after transplantation into a rat model of traumatic brain injury. J Neurosurg 2004;100:88–96.

37. Yang L, Xia Y, Zhao H, et al. Magnetic resonance imaging of transplanted neural stem cells in Parkinson disease rats. J Huazhong Univ Sci Technolog Med Sci 2006;26:489–492.

38. Modo M, Beech JS, Meade TJ, et al. A chronic 1 year assessment of MRI contrast agent-labelled neural stem cell transplants in stroke. Neuroimage 2009;47(suppl 2):T133–T142.

39. Lee ES, Chan J, Shuter B, et al. Microgel iron oxide nanoparticles for tracking human fetal mesenchymal stem cells through magnetic resonance imaging. Stem Cells 2009;27:1921–1931.

40. Belayev L, Obenaus A, Zhao W, et al. Experimental intracerebral hematoma in the rat: characterization by sequential magnetic resonance imaging, behavior, and histopathology. Effect of albumin therapy. Brain Res 2007;1157:146–155.

41. Modo M, Mellodew K, Cash D, et al. Mapping transplanted stem cell migration after a stroke: a serial, in vivo magnetic resonance imaging study. Neuroimage 2004;21:311–317.

42. Coggeshall RE, Lekan HA. Methods for determining numbers of cells and synapses: a case for more uniform standards of review. J Comp Neurol 1996;364:6–15.

43. Guillery RW, Herrup K. Quantification without pontification: choosing a method for counting objects in sectioned tissues. J Comp Neurol 1997;386:2–7.

44. Modo M, Cash D, Mellodew K, et al. Tracking transplanted stem cell migration using bifunctional, contrast agent-enhanced, magnetic resonance imaging. Neuroimage 2002;17:803–811.

45. Weber A, Pedrosa I, Kawamoto A, et al. Magnetic resonance mapping of transplanted endothelial progenitor cells for therapeutic neovascularization in ischemic heart disease. Eur J Cardiothorac Surg 2004;26:137–143.

46. Jendelova P, Herynek V, Urdzikova L, et al. Magnetic resonance tracking of human CD34+ progenitor cells separated by means of immunomagnetic selection and transplanted into injured rat brain. Cell Transplant 2005;14:173–182.

47. Flexman JA, Cross DJ, Kim Y, Minoshima S. Morphological and parametric estimation of fetal neural stem cell migratory capacity in the rat brain. Conf Proc IEEE Eng Med Biol Soc 2007;2007: 4464–4467.

48. Zhang RL, Zhang L, Zhang ZG, et al. Migration and differentiation of adult rat subventricular zone progenitor cells transplanted into the adult rat striatum. Neuroscience 2003;116:373–382.

49. Zhang ZG, Jiang Q, Zhang R, et al. Magnetic resonance imaging and neurosphere therapy of stroke in rat. Ann Neurol 2003;53: 259–263.

50. Coats JS, Freeberg A, Pajela EG, et al. Meta-analysis of apparent diffusion coefficients in the newborn brain. Pediatr Neurol 2009; 41:263–274.

51. Leppert IR, Almli CR, McKinstry RC, et al. T(2) relaxometry of normal pediatric brain development. J Magn Reson Imaging 2009;29: 258–267.

52. Jeyakumar M, Lee JP, Sibson NR, et al. Neural stem cell transplantation benefits a monogenic neurometabolic disorder during the symptomatic phase of disease. Stem Cells 2009;27:2362–2370.

53. Wang L, Martin DR, Baker HJ, et al. Neural progenitor cell transplantation and imaging in a large animal model. Neurosci Res 2007;59:327–340.

54. Yu D, Neeley WL, Pritchard CD, et al. Blockade of peroxynitrite-induced neural stem cell death in the acutely injured spinal cord by drug-releasing polymer. Stem Cells 2009;27:1212–1222.